ARTICLE

Check for updates

Vitamin D receptor upregulates tight junction protein claudin-5 against colitis-associated tumorigenesis

Yongguo Zhang[1], Shari Garrett[1,2], Robert E. Carroll[1], Yinglin Xia[1] and Jun Sun[1,2,3,4]✉

Tight junctions are essential for barrier integrity, inflammation, and cancer. Vitamin D and the vitamin D receptor (VDR) play important roles in colorectal cancer (CRC). Using the human CRC database, we found colonic VDR expression was low and significantly correlated with a reduction of Claudin-5 mRNA and protein. In the colon of $VDR^{\Delta IEC}$ mice, deletion of intestinal VDR led to lower protein and mRNA levels of Claudin-5. Intestinal permeability was increased in the $VDR^{-/-}$ colon cancer model. Lacking VDR and a reduction of Claudin-5 are associated with an increased number of tumors in the $VDR^{-/-}$ and $VDR^{\Delta IEC}$ mice. Furthermore, gain and loss functional studies have identified *CLDN-5* as a downstream target of VDR. We identified the Vitamin D response element (VDRE) binding sites in a reporter system showed that VDRE in the Claudin-5 promoter is required for vitamin D_3-induced *Claudin-5* expression. Conditional epithelial VDR overexpression protected against the loss of Claudin-5 in response to inflammation and tumorigenesis in vivo. We also reported fecal VDR reduction in a colon cancer model. This study advances the understanding of how VDR regulates intestinal barrier functions in tumorigenesis and the possibility for identifying new biomarker and therapeutic targets to restore VDR-dependent functions in CRC.

Mucosal Immunology (2022) 15:683–697; https://doi.org/10.1038/s41385-022-00502-1

INTRODUCTION

Tight junction structures are essential in intestinal innate immunity and barrier functions. The disruption of TJs is a common manifestation of various diseases, including chronic inflammation and cancers. Changes in expression and distribution of TJ proteins such as Claudin-2, −5, and −8 lead to discontinuous TJs and barrier dysfunction in active Crohn's disease (CD), a type of inflammatory bowel disease[1]. Claudin-5 is expressed in the epithelia and endothelia and form paracellular barriers and pores that determine permeability. This protein is downregulated in colon cancer[2,3].

VDR is a nuclear receptor that mediates most known functions of the biologically active form of vitamin D[4–6]. VDR possesses multiple critical roles in regulating innate and adaptive immunity, intestinal homeostasis, host response to microbiota, and tight junction structure[7–14]. Vitamin D/VDR deficiency has been implicated in patients with inflammatory bowel disease and colon cancer[15–21]. Our study demonstrated that VDR is essential for maintaining intestinal and microbial homeostasis[22], and protecting against intestinal tumorigenesis[23,24]. Although vitamin D has been extensively studied, many critical questions about the biological functions of intestinal VDR in CRC remain unanswered. Although VDR and TJ proteins (e.g., Claudins) are involved in colon cancer, it remains unclear if they are closely related or function independently. Considering the multiple functional roles of VDR in the development of colon cancer[20,24], it is important to dissect the cellular and molecular mechanisms by which VDR contributes to barrier function in protecting the host from tumorigenesis.

Here, we revisited the human CRC database and determined that colonic VDR expression is low and positively correlated with the reduction of the TJ protein Claudin-5 in CRC, including colitis-associated colon cancer. We investigate the novel role of VDR in regulating Claudin-5 expression using $VDR^{-/-}$ and intestinal epithelial VDR knockout mice ($VDR^{\Delta IEC}$) in a colitis-associated colon cancer model. Human organoids, human colon cancer samples, $VDR^{-/-}$ mouse embryonic fibroblasts (MEF) cells, and cultured intestinal epithelial cells were used to determine the molecular mechanism. We determined that VDR is an important transcriptional regulator for maintaining physiological levels of the target gene *Claudin-5* in the intestine. Furthermore, we generated a conditional intestinal epithelial VDR- overexpressed mouse model to study the protective role of VDR in the maintenance of TJs in the context of inflammation and tumorigenesis. Our goal is to provide a detailed understanding of how VDR status contributes to intestinal inflammation and cancer. Our finding may offer an additional avenue to treat colon cancer by restoring the barrier functions and developing a new protocol for risk assessment and prevention of cancer.

RESULTS

Reduced VDR was positively correlated with low Claudin-5 expression in CRC patients

We first examined the gene expression levels of VDR and Claudin-5 in normal and human CRC samples by reviewing the GEO

[1]Department of Medicine, College of Medicine, University of Illinois at Chicago, Chicago, IL, USA. [2]Department of Microbiology/Immunology, College of Medicine, University of Illinois at Chicago, Chicago, IL, USA. [3]UIC Cancer Center, University of Illinois at Chicago, Chicago, IL, USA. [4]Jesse Brown VA Medical Center, Chicago, IL, USA.
✉email: junsun7@uic.edu

Received: 3 May 2021 Revised: 28 January 2022 Accepted: 21 February 2022
Published online: 25 March 2022

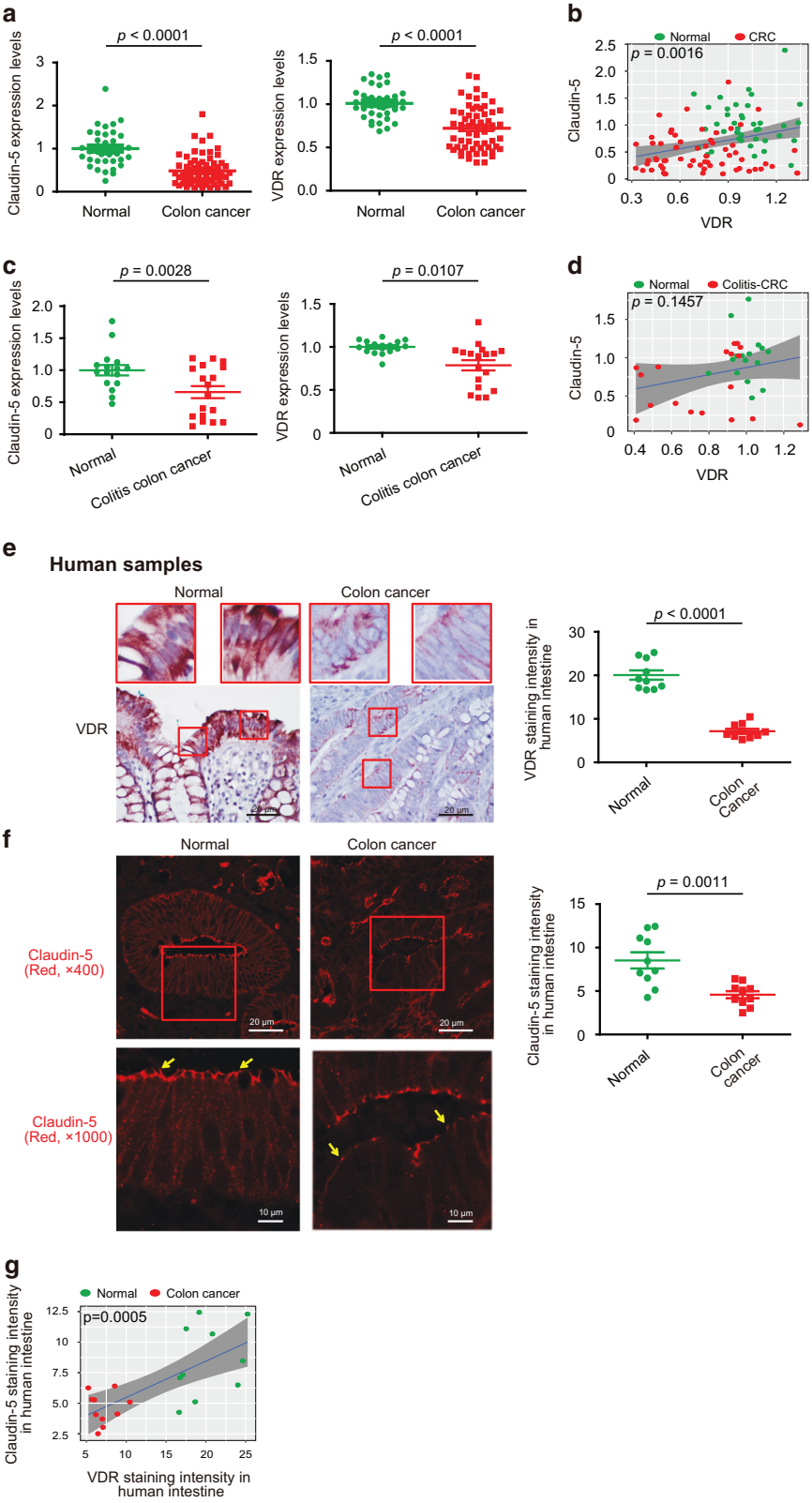

database GSE 4183 and GSE 8671 from Affymetrix data (human genome U133 Plus 2.0 arrays). Reduced VDR and Claudin-5 expression was observed in patients with CRC (Fig. 1a). To quantify and visualize the correlations between intestinal Claudin-5 and the VDR protein, we performed a correlation analysis between VDR and Claudin-5 and conducted a scatter plot with a regression line (Fig. 1b). We found significantly coordinated expression of VDR and Claudin-5 in biopsy samples collected from patients with CRC. We further analyzed data obtained from human colitis-associated colon cancer (Fig. 1c). VDR and Claudin-5 expression

Fig. 1 Reduced VDR was correlated with low Claudin-5 expression in human colorectal cancer (CRC) patients. a Reduced VDR and Claudin-5 expression in patients with CRC (GEO database GSE4183 and GSE8671, (data were expressed as mean ± SD; Normal, $n = 40$; CRC, $n = 62$; Student's t test). All p values are shown in the figure. **b** Significantly coordinated (the Pearson correlation coefficient is 0.3083 with p value = 0.001621) expression of VDR and Claudin-5 in biopsy samples collected from CRC patients. We performed a regression of VDR against Claudin-5 and conducted a scatter plot analysis with a regression line (GEO database GSE4183 and GSE8671, Normal, $n = 40$; CRC, $n = 62$; Intercept = 0.244; Slope = 0.5297). Values for healthy controls are presented in blue, and values for CRC patients are presented in red. **c** Reduced VDR and Claudin-5 expression in patients with Colitis-associated CRC (GEO database GSE8671, GSE10714 and GSE37283, data were expressed as mean ± SD; Normal, $n = 16$; Colitis-associated CRC, $n = 18$; Student's t test). **d** Coordinated expression of VDR and Claudin-5 in biopsy samples collected from Colitis-associated CRC patients. We performed a regression of VDR against Claudin-5 and conducted a scatter plot analysis with a regression line (GEO database GSE8671, GSE10714, and GSE37283 Normal, $n = 16$; Colitis-associated CRC, $n = 18$; the Pearson correlation coefficient is 0.2549 with p value = 0.1457). **e** Intestinal VDR staining in normal and CRC human colon samples. Compared with normal intestines, the intestine from CRC patients possessed significantly lower VDR expression. (Images are representative of experiments performed in triplicate; Normal, $n = 10$; Colorectal cancer, $n = 10$; Student's t test). **f** IF staining of Claudin-5 in normal and CRC human colon samples. Compared to normal intestines, the intestines of CRC patients exhibited significantly lower Claudin-5 expression. (Images are representative of experiments in triplicate; Normal, $n = 10$; Colon cancer, $n = 10$; Student's t test). **g** The Pearson correlation analysis of staining intensity between intestinal Claudin-5 and VDR in human colon samples (the Pearson correlation coefficient is 0.7033 with p value = 0.0005417. $n = 10$ for Normal and Colon cancer, respectively). All p values are shown in this figure.

was significantly reduced in patients with colitis-associated CRC (GEO database GSE8671, GSE10714, and GSE37283) (Fig. 1c). We identified a positive correlation between VDR and Claudin-5 in biopsy samples collected from colitis-associated CRC patients and healthy controls (Fig. 1d). We then examined the protein levels of intestinal VDR in normal and CRC human colon samples using IHC. Compared to normal intestines, CRC patients with CRC possessed significantly lower VDR expression (Fig. 1e). Immunofluorescence (IF) staining of Claudin-5 revealed significantly lower Claudin-5 expression in CRC human colon samples (Fig. 1f). We performed correlation analysis and scatter plot of the staining intensity changes between the VDR protein and Claudin-5 in the colon. The results revealed that the staining intensity of Claudin-5 and intestinal VDR was positively associated with the Pearson correlation analysis (Fig. 1g). Thus, we revealed that colonic VDR expression is low and is correlated with the reduction of Claudin-5 at both mRNA and protein levels in human CRC, including colitis-associated colon cancer.

Larger and more tumors developed in VDR deficient mice

Animal models have been developed to reflect the initiation and progression of human colon cancer[25]. Azoxymethane (AOM)[26] mice develop hyperproliferative colonic mucosa, aberrant crypt foci, and eventually carcinomas[27]. An AOM-dextran sulfate sodium[28] model is widely used to study colitis-associated colon cancer[29]. We next investigated the role of VDR in regulating Claudin-5 expression in the development of cancer using an AOM/DSS treated mouse models (Fig. 2a). For wild-type $VDR^{+/+}$ and whole body VDR knockout ($VDR^{-/-}$) mice, representative colons with tumors are shown (Fig. 2b). We observed that AOM/DSS-treated $VDR^{-/-}$ mice developed more tumors in the colon (Fig. 2c). The maximum tumor size was significantly larger in $VDR^{-/-}$ mice than in $VDR^{+/+}$ mice (Fig. 2d). Furthermore, pathological analysis of colon samples indicated differences in tumor stage (carcinoma versus adenoma) between $VDR^{-/-}$ mice and the $VDR^{+/+}$ AOM/DSS experimental groups (Fig. 2e). Epithelial hyperproliferation plays a critical role in the development of cancer. The IF data of the proliferative marker PCNA revealed that PCNA in the colon was significantly increased in the $VDR^{-/-}$ mice compared to that in the $VDR^{+/+}$ mice (Fig. 2f). Chronic inflammation is one of the factors that contribute to CRC. We determined that serum cytokines TNF-α, IL-1β, and IL17 were significantly higher in the $VDR^{-/-}$ mice, compared to the $VDR^{+/+}$ mice (Fig. 2g).

VDR deletion leads to decreased Claudin-5 expression in tumor tissues

We examined changes in barrier function by testing intestinal permeability in mice with or without tumors. Mice were gavaged with fluorescein dextran (Molecular weight 3 kDa). After 4 h, blood samples were collected for fluorescence intensity measurement. Higher fluorescence intensity is indicative of higher intestinal permeability. As shown in Fig. 3a, AOM/DSS treatment increased intestinal permeability in both $VDR^{+/+}$ and $VDR^{-/-}$mice, while the $VDR^{-/-}$ mice exhibited significantly higher permeability post-treatment. Based on the in vivo intestinal permeability data, we hypothesized that the TJ proteins would be altered in the AOM/DSS mice. In the $VDR^{-/-}$ mice, we observed significant down-regulation of Claudin-5 at the mRNA and protein levels in the colon (Fig. 3b and c). In the basal condition, Claudin-2 expression was decreased in $VDR^{-/-}$ mice, compared to the $VDR^{+/+}$ mice. However, there was no difference in the tumor tissues between $VDR^{+/+}$ and $VDR^{-/-}$ mice. The tight junction protein Claudin-7 did not show any changes either (Fig. 3c). Claudin-5 staining was observed at the crypt surface and at the lower portion of the intestine. Reduced Claudin-5 expression was confirmed through the immunostaining of colon tissues in the AOM/DSS mice (Fig. 3d and g). However, VDR deletion did not alter the expression of the TJ protein Claudin-7 in the colon of $VDR^{-/-}$ mice, compared to that of $VDR^{+/+}$ mice (Fig. 3e). VDR expression was also decreased in mice with AOM/DSS-induced colon cancer (Fig. 3f and h). Moreover, we used our recently established method to measure VDR levels according to qPCR in fecal samples[30]. We detected a significant reduction in VDR in fecal samples from mice with tumors (Fig. 3i). These data also suggest a decreased VDR in epithelial cells shed from mice with tumors.

Conditional deletion of intestinal epithelial VDR led to increased permeability and reduced clauidn-5 in the AOM/DSS cancer model

To understand the tissue-specific role of Claudin-5 in colon cancer, we further studied intestinal permeability and Claudin-5 using a conditional intestinal epithelial VDR deletion $VDR^{\Delta IEC}$ model by fluorescein dextran measurement. We found that intestinal permeability indicated by the serum fluorescence intensity was significantly increased in $VDR^{\Delta IEC}$ mice (Fig. 4a). Intestinal epithelial VDR specific deletion led to significantly decreased Claudin-5 at the mRNA level in the colon (Fig. 4b) and further decreased in the mice with colon cancer. However, Claudin-2 was decreased in the $VDR^{\Delta IEC}$ mice, compared to the VDR^{loxp} mice at the basal condition, but not decreased in the tumor tissues of $VDR^{\Delta IEC}$ and VDR^{loxp} mice. Claudin-7 was not altered in the absence of VDR. At the protein level, we found reduced Claudin-5 in the $VDR^{\Delta IEC}$ mice (Fig. 4c). In tumor tissues of $VDR^{\Delta IEC}$ mice, epithelial Claudin-5 was disorganized and significantly decreased (Fig. 4d), compared to that in tumors of VDR^{loxp} mice (Fig. 4f). In contrast, Claudin-7 was not altered in tumors from $VDR^{\Delta IEC}$ mice compared to the tumor tissue of VDR^{loxp} mice (Fig. 4e). The VDR expression in fecal samples was down-regulated in the AOM-DSS VDR^{loxp} mice (Fig. 4g).

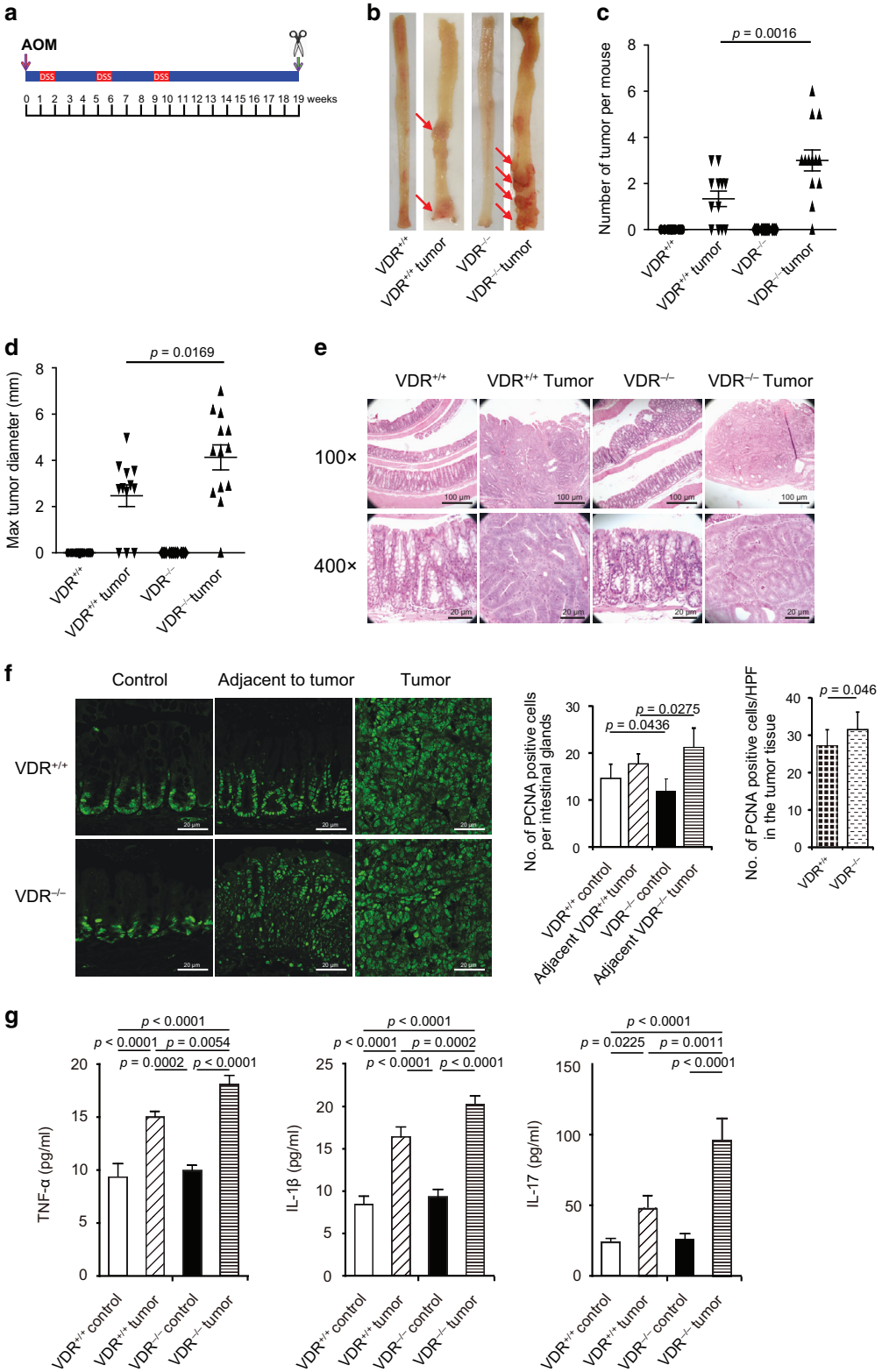

Identification of the vitamin D-response element (VDRE) in the Claudin-5 promoter

To confirm the direct regulation of VDR on Claudin-5, we examined various models at the basal level without any treatment in vivo and in vitro. In the $VDR^{-/-}$ mice, we observed that these mice possessed lower Claudin-5 protein levels in the colon than did $VDR^{+/+}$ mice, and TJ Claudin-7 was not altered in the absence of VDR (Fig. S1A). We further detected significantly decreased mRNA levels of Claudin-5 in the intestine of $VDR^{-/-}$ mice (Fig. S1B). The density of Claudin-5 fluorescence staining was weaker in the $VDR^{-/-}$ mouse intestines (Fig. S1C). We also checked the specificity of intestinal VDR in regulating Claudin-5

Fig. 2 $VDR^{-/-}$ mice developed a greater number of tumors compared to tumors in $VDR^{+/+}$ mice. a Schematic overview of the AOM/DSS-induced colon cancer model. AOM (10 mg/kg) was injected on day 0. On Day 7, 2% DSS solution was administered to mice in drinking water. Seven days of DSS was followed by 3 weeks of drinking water free of DSS. An additional two cycles of DSS were administered prior to sacrifice at Week 19. **b** Colonic tumors in situ. Representative colons from different groups. Tumors were indicated by red arrows. **c** Tumor number in AOM-DSS induced colon cancer model: $VDR^{+/+}$ and $VDR^{-/-}$ mice (data are expressed as mean ± SD. $n = 10–13$, one-way ANOVA test). **d** Max tumor size in AOM-DSS induced colon cancer model: $VDR^{+/+}$ and $VDR^{-/-}$ mice (data are expressed as mean ± SD. $n = 10–13$, one-way ANOVA test). **e** Representative H&E staining of "Swiss rolls" of representative colons from the indicated groups. Images are from a single experiment and represent ten mice per group. **f** Quantitation of PCNA-positive cells in control mucosa per intestinal glands or in the tumors tissue per high-power field. PCNA expression in the tumor tissue of $VDR^{-/-}$ mice was significantly higher than that in the $VDR^{+/+}$ mice (data are expressed as mean ± SD. $n = 5$, Student's t test). **g** Serum cytokines such as TNF-α, IL-1β, and IL-17 were significantly increased, particularly in the AOM-DSS-induced $VDR^{-/-}$ mice colon cancer model. Each single experiment was assayed in triplicate. Data are expressed as mean ± SD. $n = 6$, one-way ANOVA test. All p values are shown in the figure.

expression in $VDR^{\Delta IEC}$ mice (Fig. S1D). Claudin-5 mRNA levels were significantly reduced in $VDR^{\Delta IEC}$ mice compared to those in VDR-lox mice (Fig. S1E). As expected, Claudin-7 expression remained unchanged. These data indicated that intestinal VDR specifically regulates the expression level of Claudin-5 in the colon. To confirm our finding in vitro, we used MEFs with VDR deletion. Lack of VDR led to a robust decrease of Claudin-5 at protein and mRNA levels in $VDR^{-/-}$ MEFs at the basal level (Fig. S1F and G). The density of Claudin-5 fluorescence staining was also weaker in the $VDR^{-/-}$ MEFs (Fig. S1H).

VDR acts as a transcription factor to regulate the expression of its target genes[31,32]. Activated VDR binds to the VDRE in the target gene promoter to regulate gene transcription[33]. We reasoned that VDR might bind to the *Claudin-5* promoter,thus altering the mRNA expression of the Claudin-5 gene. Further, we performed ChIP assay using the colon mucosal extract from $VDR^{-/-}$ mice and nonspecific IgG as a negative control to assess the binding of VDR to the Claudin-5 promoter. The samples were amplified by conventional PCR with Ikβα as positive control and Claudin-1 as a negative control as indicated in previous publications[34]. CHIP-PCR demonstrated that VDR binds to the Claudin-5 promoter in the $VDR^{+/+}$ mouse colon (Fig. 5a). The VDRE sequence (AGTTTGGTTGTGGGCT) within the Claudin-5 promoter region is shown in Fig. 5b. We next assessed whether vitamin D3 could enhance Claudin-5 promoter activity through the VDRE binding sites. DNA sequences in the promoter region of vitamin D regulated genes were used in an in vitro reporter luciferase assay. A schematic drawing of transcriptional binding sites in the WT Claudin-5 promoter and its mutants are shown in Fig. 5c & Fig. S2. Plasmids with WT or deletions of VDRE, D2, or D3 in the Claudin-5 promoter binding were transfected into human SKCO15 cells, respectively followed by vitamin D_3 treatment. We found Vitamin D_3 enhanced WT-Claudin-5 promoter activity in cells. Deletions of D2 and D3 binding sites did not affect the Claudin-5 promoter activity. In contrast, deletions of VDRE binding sites clearly suppressed the promoter activity (Fig. 5d). These results demonstrate that the binding of VDRE binding sites in the Claudin-5 promoter is required for vitamin D_3-induced Claudin-5 expression. However, siRNA-based Claudin-5 knockdown did not reduce VDR expression at the mRNA level (Fig. 5e). At the protein level, reduced Claudin-5 did not change the status of VDR protein or Claudin-7 at the protein level (Fig. 5f). Together, these results suggest that VDR transcriptionally regulates Claudin-5 at the mRNA level and that VDR is the upstream regulator of Claudin-5.

High VDR levels led to increased Claudin-5 protein and mRNA levels in vitro

We then explored the possibility of enhancing VDR to maintain the physiological level of Claudin-5. Vitamin D3 is known to increase VDR expression and activate VDR signaling. We used the human colonic epithelial SKCO15 cell line that is widely used in studying TJs[35,36]. Claudin-5 mRNA level was significantly elevated in SKCO15 cells treated with Vitamin D3, whereas Claudin-7 mRNA was not altered by vitamin D3 treatment (Fig. 6a). The protein level of Claudin-5 and Claudin-2 were induced by Vitamin D3 (Fig. 6b). In vivo, Claudin-5 mRNA and protein levels were also increased in vitamin D3-treated mice (Fig. 6c and d). The protein level of Claudin-2 was also increased in vitamin D3-treated mice. (Fig. 6d). Colonoids are three-dimensional (3D) cell cultures that incorporate some of the key features of the represented organ[37]. In this study, we developed human colonoids (Fig. 6e), and we observed vitamin D3 treatment significantly increased Claudin-5 mRNA level in these colonoids (Fig. 6f). Furthermore, vitamin D3 treatment significantly increased Claudin-5 and Claudin-2 protein levels in human colonoids, whereas there was no change of Claudin-7 after vitamin D3 treatment (Fig. 6g).

Intestinal epithelial VDR overexpression protected against the loss of Claudin-5 in respond to intestinal inflammation

To further investigate the protective role of VDR in maintaining TJs in inflammation, we used a conditional intestinal epithelial VDR specific-overexpressed (O-VDR) mouse model generated in our previous study[38]. Epithelial VDR overexpression in mouse intestines significantly increased Claudin-5 expression at both the mRNA and protein levels (Fig. 7a and b). Claudin-5 exhibited a minor decrease at the mRNA and protein levels in the colon of O-VDR mice treated with DSS, compared to that in the $O\text{-}VDR^{loxp}$ mice (Fig. 7c and d). Using IF staining, we determined that Claudin-5 was better preserved in the colon of O-VDR mice treated with DSS compared to that in the $O\text{-}VDR^{loxp}$ mice (Fig. 7e and g). As anticipated, Claudin-7 expression was unchanged in the intestinal tissue of O-VDR mice treated with DSS compared to that in the $O\text{-}VDR^{loxp}$ mice (Fig. 7f). VDR levels in fecal samples were detected using RT-PCR. VDR levels had a minor decrease in DSS-treated O-VDR mice, compared to that in $O\text{-}VDR^{loxp}$ mice treated with DSS (Fig. 7h). Moreover, there were fewer inflammatory cytokines such as IL-1β and IL-17 in the colons of DSS-induced O-VDR mice compared to $O\text{-}VDR^{loxp}$ mice (Fig. 7i).

Overexpressed intestinal epithelial VDR mice had less and smaller tumors in the AOM/DSS colon cancer model

The role of overexpression intestinal epithelial VDR was further examined in the development of colon cancer using an AOM/DSS model. Figure 8a showed the tumors in the colon of representative $O\text{-}VDR^{loxp}$ and O-VDR mice. We observed that AOM/DSS-treated O-VDR mice developed fewer tumors than $O\text{-}VDR^{loxp}$ mice (Fig. 8b). The tumor size was significantly smaller in O-VDR mice than in $O\text{-}VDR^{loxp}$ mice (Fig. 8c). Claudin-5 exhibited a minor decrease at the mRNA and protein levels in the tumor tissue of O-VDR mice, compared to that in the tumors from $O\text{-}VDR^{loxp}$ mice (Fig. 8d and e). Moreover, there were fewer inflammatory cytokines, such as IL-1β and IL-17, in the tumor tissue of AOM/DSS-induced O-VDR mice, than those in $O\text{-}VDR^{loxp}$ mice (Fig. 8f).

DISCUSSION

In the current study, we determined that low colonic VDR expression was significantly correlated with the reduction of

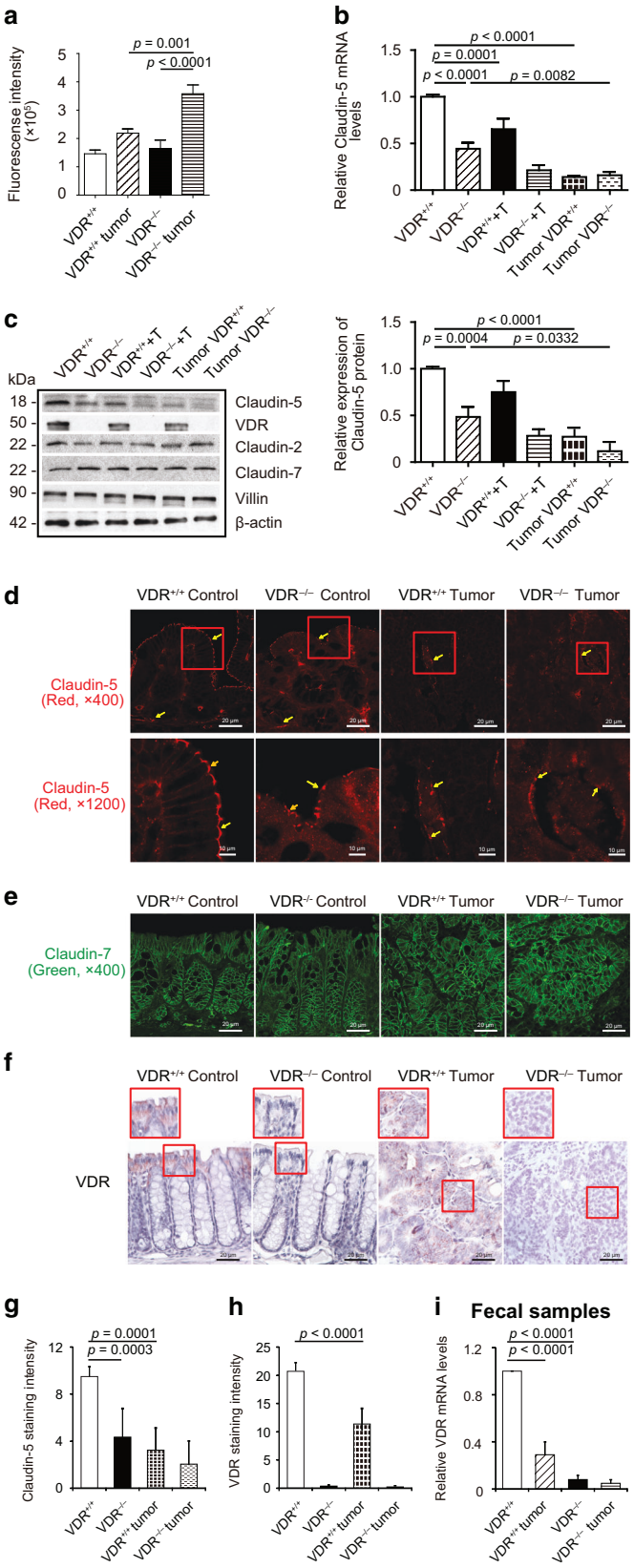

Fig. 3 VDR deletion led to decreased Claudin-5 expression in tumor tissues. a Intestinal permeability increased in the AOM-DSS-induced $VDR^{-/-}$ mice colon cancer model. Fluorescein Dextran (Molecular weight 3 kDa, diluted in HBSS) was gavaged (50 mg/g mouse). Four hours later, mouse blood samples were collected for fluorescence intensity measurement (data are expressed as mean ± SD; $n = 5$ mice/group, 1-way ANOVA test). **b** VDR deletion decreased Claudin-5 at the mRNA level in the colon (data are expressed as mean ± SD. $n = 5$, one-way ANOVA test). **c** VDR deletion decreased Claudin-5 at the protein levels in the colon (data are expressed as mean ± SD. $n = 5$, one-way ANOVA test). Claudin-2 was decreased in the $VDR^{-/-}$ mice, compared to $VDR^{+/+}$ mice in the basal condition, but there was no difference between the tumor tissue of $VDR^{+/+}$ and $VDR^{-/-}$ mice. **d** and **g** Claudin-5 was decreased in the tumor tissue of $VDR^{-/-}$ mice, compared to levels in the tumor tissue of $VDR^{+/+}$ mice according to immunofluorescence staining. Images are from a single experiment and represent 6 mice per group. (Data are expressed as mean ± SD. $n = 6$, one-way ANOVA test). **e** Claudin-7 was unchanged in the tumor tissue of $VDR^{-/-}$ mice, compared to levels in the tumor tissue of $VDR^{+/+}$ mice according to immunofluorescence staining. Images are from a single experiment and represent 6 mice per group. **f** and **h** Intestinal VDR expression was decreased in the AOM-DSS-induced colon cancer model. Images are from a single experiment and represent six mice per group. (Data are expressed as mean ± SD. $n = 6$, one-way ANOVA test). **i** VDR levels in fecal samples were detected using RT-PCR. VDR expression was downregulated in the AOM-DSS-treated $VDR^{+/+}$ mice (data are expressed as mean ± SD. $n = 5$, one-way ANOVA test). All p values are shown in this figure.

Claudin-5 in human CRC. We demonstrated that VDR is important for maintaining cellular and physiological levels of TJ protein Claudin-5 in the colon to prevent inflammation and tumorigenesis. Our study further revealed a complex role for vitamin D/VDR regulation of *CLDN-5* in the development of colon cancer. Lacking VDR reduced Claudin-5 in tumors, and enhanced VDR increased Claudin-5 to protect the intestinal epithelial cells from tumorigenesis. At the molecular level, our data have demonstrated that the *CLDN-5* gene is a newly discovered downstream target of the transcriptional factor VDR. Overall, we noted a link between VDR signaling and barrier functions in CRC, thus suggesting a potential biomarker and target for a novel therapeutic strategy. Our study provides insight into how VDR signaling is involved in the tissue barrier related to tumorigenesis.

The intestinal barrier includes several elements that aid in its function as a physical and immunological barrier. These elements include the intestinal microbiota, secretory immunoglobulin A, antimicrobial peptides, the inner lamina propria, and epithelial cells. Epithelial cells play physical and physiological roles in health and disease at the cellular level. VDR signaling is involved in the epithelial barrier function related to various human diseases and remains largely unexplored[39]. As a nuclear receptor, VDR mediates most known functions of 1,25-dihydroxyvitamin D ($1,25(OH)_2D_3$), the active form of vitamin D[4]. However, the role of VDR has rarely been evaluated in studies examining human colon cancer. A recent study among patients with digestive tract cancer and vitamin D supplementation determined that when compared to placebo, this treatment did not result in significant improvement in relapse-free survival at 5 years[40]. The dosage of vitamin D3 was insufficient among participants who possessed more severe deficiency at baseline. Therefore, the status of the VDR level must be considered over the course of many trials or as a biological measurement to clarify the underlying mechanisms. The traditional model of treatment using vitamin D that guided early vitamin studies should give way to a model incorporating more complex mechanisms of action of the Vitamin D/VDR system. Various methods have investigated the intestinal barrier, but the correlation of results across studies is difficult, representing a major shortcoming in the field[41].

The current study provides important insights into how VDR regulates Claudin-5 expression under normal physiological conditions and during tumor growth in the colon. We revealed a

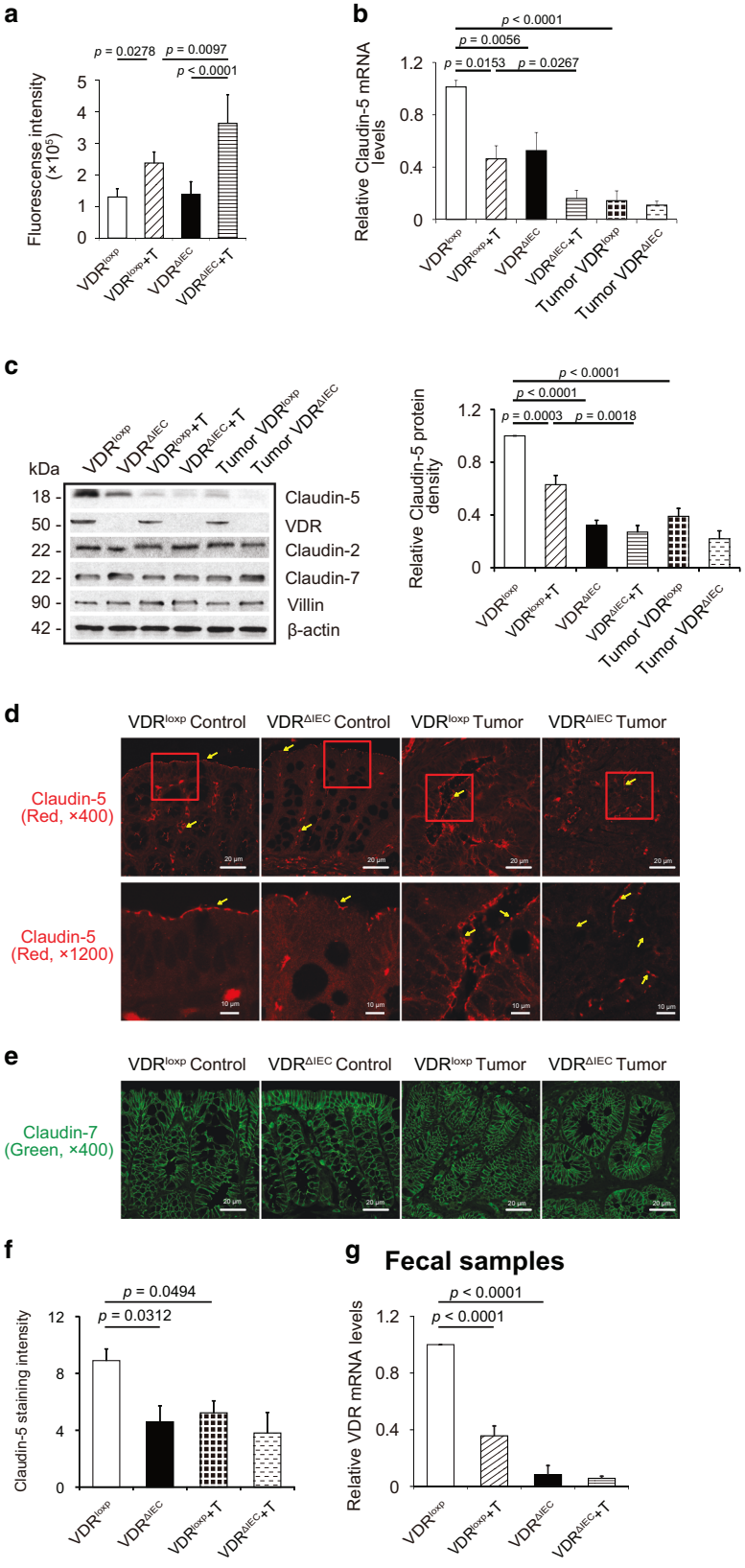

positive correlation between VDR and Claudin-5 at the mRNA and protein levels in healthy and tumor colons, thus suggesting the unique role of Claudin-5 in the intestine. There are 27 claudin family members that contribute to tight junctions[42], and not all Claudins are the same. Claudin-2 and Claudin-12 form paracellular Ca^{2+} channels in intestinal epithelia and are important for vitamin D-dependent calcium homeostasis[43]. Our previous studies have shown that Claudin-2 is hyper regulated in colitis with VDR

Fig. 4 VDR-specific deletion in mouse intestines lead to decreased Claudin-5 expression in tumor tissues. a Intestinal permeability was increased in the AOM-DSS-induce $VDR^{\Delta IEC}$ mice colon cancer model (data are expressed as mean ± SD; $n = 5$ mice/group, One-way ANOVA test). **b** VDR-specific deletion in mouse intestines decreased Claudin-5 at the mRNA level in the colon (data are expressed as mean ± SD. $n = 5$, one-way ANOVA test). **c** VDR-specific deletion in mouse intestines decreased Claudin-5 protein in the colon (data are expressed as mean ± SD. $n = 5$, one-way ANOVA test.) Claudin-2 was decreased in the $VDR^{\Delta IEC}$ mice, compared to the VDR^{loxp} mice in the basal level, but not decreased in the tumor tissue of $VDR^{\Delta IEC}$ and VDR^{loxp} mice. **d** Claudin-5 was decreased in the tumor tissue of $VDR^{\Delta IEC}$ mice compared to levels in the tumor tissue of VDR^{loxp} mice according to immunofluorescence staining. Images are from a single experiment and represent six mice per group. **e** Claudin-7 expression was not changed in the AOM-DSS-induced VDR^{loxp} mice colon cancer model. Images are from a single experiment and represent of 6 mice per group. **f** Intensity of the staining of Claudin-5. (Data are expressed as mean ± SD. $n = 6$, one-way ANOVA test). **G** VDR level in fecal samples was detected by RT-PCR. VDR expression was downregulated in the AOM-DSS-treated VDR^{loxp} mice (data are expressed as mean ± SD. $n = 3$, one-way ANOVA test). All p values are shown in the figure.

reduction[34,44]. Our current study has demonstrated the mechanism of the VDR-dependent function of Claudin-5 in the intestine. Interestingly, we found that the tight junction Claudin-7 was not altered in response to VDR-deficient status in the colon. In the lungs, VDR may play an important role in maintaining the pulmonary barrier integrity. We have reported that VDR deletion could increase lung permeability by altering the expression of TJ molecules, particularly Claudin-2, −4, −10, −12, and −18[45]. Abnormal gut barrier function may serve as a biomarker for the risk of IBD onset[46]. Our findings also suggest that the positively correlated status of VDR and Claudin-5 could be potentially applied to risk assessment, early detection, and prevention of CRC, including colitis-associated colon cancer.

Colorectal cancer (CRC) is the second-leading cause of cancer-related death and is most curable in its early stages. Targeting barrier functions and microbiome[47] has been made regarding colon cancer therapy. Our study has provided a detailed understanding of how VDR status contributes to changes in TJs in the context of intestinal inflammation and colon cancer. Currently, there are no guidelines for monitoring vitamin D status, treating hypovitaminosis D, and maintaining optimal vitamin D stores in patients with IBD[48] or CRC. These tasks may prove particularly difficult due to malabsorption, gastrointestinal losses, and increased permeability associated with intestinal dysfunction. Based on the research progress regarding the novel roles of VDR in intestinal immunity and barrier functions, we expect that studies on VDR in intestinal barriers of colitis and colon cancer will have a marked impact on the prevention, diagnosis, and therapy of colitis and colon cancer patients.

Barrier function and VDR status are not only essential for the maintenance of intestinal homeostasis, but they are also critical for the development of chronic mucosal inflammation and cancer. Gut microbiome regulate both innate and adaptive immunity of the host. A conditional deletion of the VDR in intestinal epithelial cells or immune cells led to different changes of the intestinal virome and altered viral-bacterial interactions[49]. CRC is a disease determimed by multiple factors, including host genetic backgound, immunity, environment, and microbiome[50–52]. Malfunction of the innate immune system and barrier function may promote the development of CRC. Moreover, VDR is known to protects against dysbiosis and tumorigenesi[24]. This knowledge can be used to develop intestinal VDR-associated mirobiome and Claudin-5 as clinical biomarkers for identifying patients who may benefit from currently available interventions and could also be used for the eventual development of novel strategies for the prevention and treatment of human CRC.

MATERIALS AND METHODS

Human tissue samples

This study was performed in accordance with approval from the University of Rochester Ethics Committee (RSRB00037178) and UIC Ethics Committee (Institutional Review Board: 2017-0384). Colorectal tissue samples were obtained from ten CRC patients with neoplasia and ten patients without neoplasia (49–74 years old). Human tissues for organoids are from healthy volunteers.

Gene expression datasets

For expression analyses, we used microarray data reported in the NCBI Gene Expression Omnibus database (GEO). To find the correlation between VDR and Claudin-5 at the gene expression level, we gathered data by searching the GEO (https://www.ncbi.nlm.nih.gov/geo/) for expression profiling studies using colonic samples from colon cancer subjects. We randomly identified the GEO database reference series: GSE4183[53], GSE8671[54], GSE10714[55], and GSE37283[56]. In these studies, the authors performed microarray analysis using colonic biopsy samples from healthy controls as well as from the inflamed and non-inflamed colonic mucosa from CRC subjects. From the databases, 40 healthy controls and 62 CRC patients were randomly selected for the CRC group, while 16 healthy controls and 18 colitis-associated CRC were randomly selected for the colitis-associated group. Both were subjected to further analyses.

Animals

$VDR^{-/-}$ mice on a C57BL/6 background were obtained by breeding heterozygous $VDR^{+/-}$ mice[34]. $VDR^{\Delta IEC}$ mice were obtained by crossing the VDR^{loxp} mice, originally provided by Dr. Geert Carmeliet, with villin-cre mice (Jackson Laboratory, 004586), as we previously reported[23,31,57]. We further backcrossed this strain with C57BL/6 mice for more than ten generations after arriving our animal facility.

Intestinal-specific VDR-overexpressing (O-VDR) mice were generated in C57BL/6 mice strain background, as reported in our recent study[38]. The mouse VDR (mVDR) sequence was cloned into the Stbl3 vector (size 6631 bp). The mVDR was cloned in (from ~2210 bp to ~3316 bp) under EF1A promoter (1–1105 bp). A LoxP site was integrated after EF1A promoter (from 1105 to 2210 bp). VDR expression in O-VDR mice is Cre driven[38]. This $O\text{-}VDR^{loxp}$ mouse line is labeled as $O\text{-}VDR^{loxp}$ in our gain of function study, distinct from the VDR^{loxp} mouse made for $VDR^{\Delta IEC}$ mice.

Experiments were performed on 2–3 months old mice, including male and female. Mice were provided with water ad libitum and maintained in a 12 h dark/light cycle. The animal work was approved by the Rush University Animal Resources committee and UIC Office of Animal Care. The animal work was approved by the UIC Office of Animal Care (ACC 15-231,17-218, and 18-216).

Induction of colon cancer by AOM-DSS in mice

Mice were treated with 10 mg/kg of AOM (Sigma-Aldrich, Milwaukee, WI, USA) by intraperitoneal injection as previously described[24]. After a 7-day recovery period, mice received three cycles of 2% DSS in the drinking water. Tumor counts and measurements were performed in a blinded fashion under a stereo-dissecting microscope (Nikon SMZ1000, Melville, NY, USA). Microscopic analysis was performed for the severity of inflammation and dysplasia on hematoxylin and eosin-stained 'Swiss rolled' colons by a gastrointestinal pathologist blinded to treatment conditions. Mice were scarified under anesthesia.

Induction of colitis and experimental design

Eight- to ten-week-old mice of a specific genetic background were grouped randomly into control and DSS treatment groups. Colitis was induced by adding 5% (weight/volume) dextran sodium sulfate[28] (mol. wt 36–50 kD; USB Corporation, Cleveland, OH, USA) to the drinking water for 7 days. Mice were monitored regularly, and their body weights were noted every day. All mice were provided a regular chow diet ad libitum. We checked the effect of DSS on both OVDR mice and compared them with their respective control group. On day 7, mice were sacrificed, and intestinal tissue and blood samples were harvested for RNA, protein, IF,

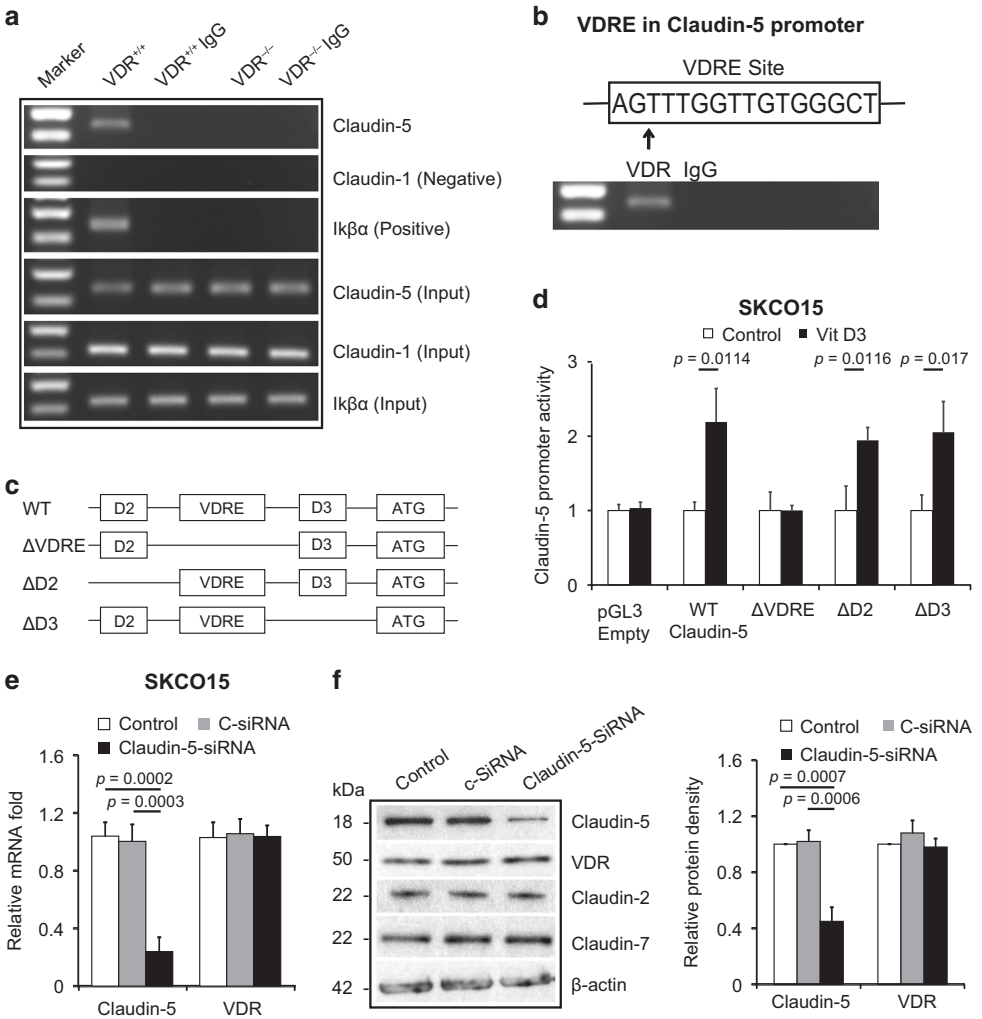

Fig. 5 VDR binds to the Claudin-5 promoter in vivo and in vitro. a CHIP-PCR amplification demonstrated that VDR binds to the promoter regions of Claudin-5 in mouse colons. PCR assays were performed and included input-positive controls and IgG/villin-negative controls. $n = 3$ separate experiments. **b** Claudin-5 promoter regions with VDRE sequence. **c** A schematic representation of transcriptional binding sites in the WT Claudin-5 promoter and deletion mutants. Plasmids include WT, binding site deletions of ΔVDRE, ΔD2, or ΔD3 in the Claudin-5 promoter. D2 and D3 domain were randomly selected upstream and downstream of the VDRE domain. **d** WT Claudin-5 reporter gene plasmids and the deletion mutant plasmids were transfected to SKCO15 cells. Luciferase activity was measured in the cell monolayers incubated in the absence or presence of vitamin D_3 (20 nM) for 24 h (data are expressed as mean ± SD. $n = 3$, Student's t test). **e** Claudin-5 knockdown using siRNA (40 nM for 72 h) did not reduce VDR expression at the mRNA level (data are expressed as mean ± SD. $n = 3$, one-way ANOVA test). **f** The protein expression in SKCO15 cells using siRNA (40 nM for 72 h) (data are expressed as mean ± SD. $n = 3$, one-way ANOVA test). All p values are shown in the figure.

and cytokine analysis, as described in the results section. The samples were immediately frozen and kept at −80 °C until use.

Vitamin D3 treatment in vivo

C57/BL/6 wild-type mice (6–8-week-old males and females) were gavaged with 1,25 D_3 (0.2 µg/day in 100 µl of corn oil) three times a week for 4 weeks, as described in our previous study[58]. Intestinal tissue was collected following euthanasia.

Cell culture

Mouse embryonic fibroblasts (MEF) were isolated from embryonic day 13.5 embryos generated from $VDR^{+/-}$ x $VDR^{+/-}$ mouse breeding as previously described[34]. $VDR^{+/+}$ and $VDR^{-/-}$ MEFs were used in experiments after more than 15 passages when they had been immortalized. MEFs and SKCO15 cells were grown in high glucose Dulbecco's Modified Eagle Medium (DMEM) (Hyclone, SH30243.01) containing 10% (v/v) fetal bovine serum (GEMINI, 900-108), 50 µg/ml streptomycin, and 50 U/ml penicillin (Mediatech, Inc., 30-002CI), as previously described[59].

Colonoids cultures and treatment with Vit D3

Human colonoids were prepared and maintained as previously described[60]. Mini gut medium (advanced DMEM/F12 supplemented with HEPES, L-glutamine, N2, and B27) was added to the culture, along with R-Spondin, Noggin, EGF, and Wnt-3a. On day 7 after passage, colonoids were treated by Vit D3 (20 nM) for indicated times.

Western blot analysis and antibodies

Mouse colonic epithelial cells were collected by scraping the tissue from the colon of the mouse, including the proximal and distal regions. The cells were sonicated in lysis buffer (10 mM Tris, pH 7.4, 150 mM NaCl, 1 mM EDTA, 1 mM EGTA, pH 8.0, 1% Triton X-100) with 0.2 mM sodium ortho-vanadate, and protease inhibitor cocktail. The protein concentration was measured using the BioRad Reagent (BioRad, Hercules, CA, USA). Cultured cells were rinsed twice with ice-cold HBSS, lysed in protein loading buffer (50 mM Tris, pH 6.8, 100 mM dithiothreitol, 2% SDS, 0.1% bromophenol blue, 10% glycerol), and then sonicated. Equal amounts of protein were separated by SDS-polyacrylamide gel electrophoresis, transferred to nitrocellulose, and

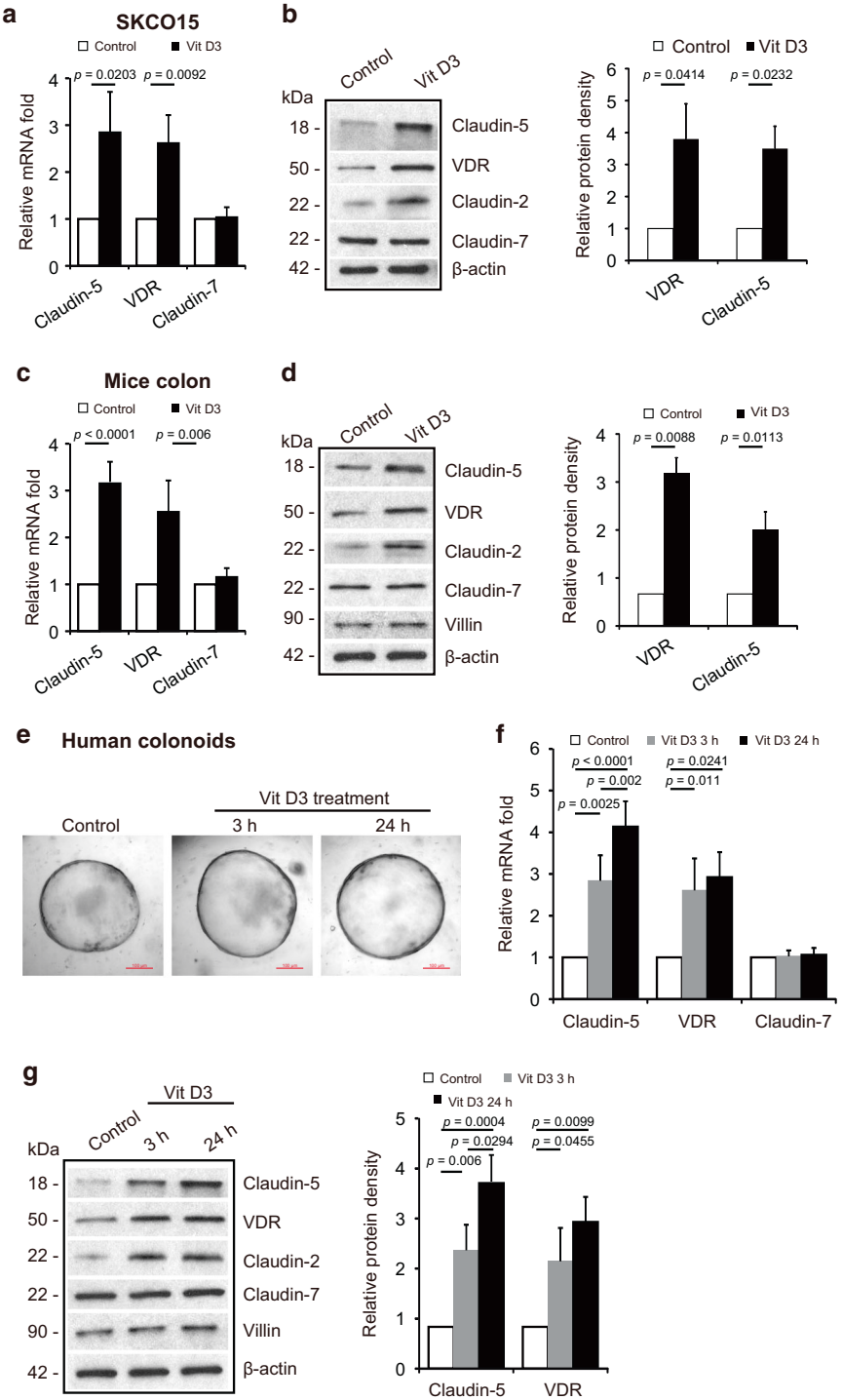

Fig. 6 High VDR levels increased Claudin-5 at the protein and mRNA level in vitro. a Claudin-5 mRNA and (**b**) protein levels were increased after 24 h vitamin D3 treatment at 20 nM in SKCO15 cells (data are expressed as mean ± SD. Student's *t* test, $n = 3$). **c** Claudin-5 mRNA and (**d**) protein levels were higher in vitamin D3- treated $VDR^{+/+}$ mice. $VDR^{+/+}$ mice (6–8 weeks) were gavaged by 0.2 µg vitamin D3 in 0.1 ml corn oil three times per week for 4 weeks (data are expressed as mean ± SD. Student's *t* test, $n = 5$ mice/group). **e** The micrographs showed representative human colonoids treated with Vit D_3 (20 nM) for the indicated time points. **f** Claudin-5 mRNA and (**g**) protein levels were increased after vitamin D3 treatment in human colonoids (data are expressed as mean ± SD, $n = 5$, one-way ANOVA test). All *p* values are shown in the figure.

immunoblotted with primary antibodies. The following antibodies were used: anti-Claudin-5 (Invitrogen, 35-2500, Carlsbad, CA, USA), anti-Claudin-7 (Invitrogen, 34-9100, Carlsbad, CA, USA), anti-VDR (Santa Cruz Biotechnology, SC-13133, Dallas, TX, USA), anti-Villin (Santa Cruz Biotechnology, SC-7672 Dallas, TX, USA), or anti-β-actin (Sigma-Aldrich, A5316, St. Louis, MO, USA) antibodies and were visualized by ECL (Thermo Fisher Scientific, 32106, Waltham, MA, USA). Membranes that were probed with more than one antibody were stripped before re-probing.

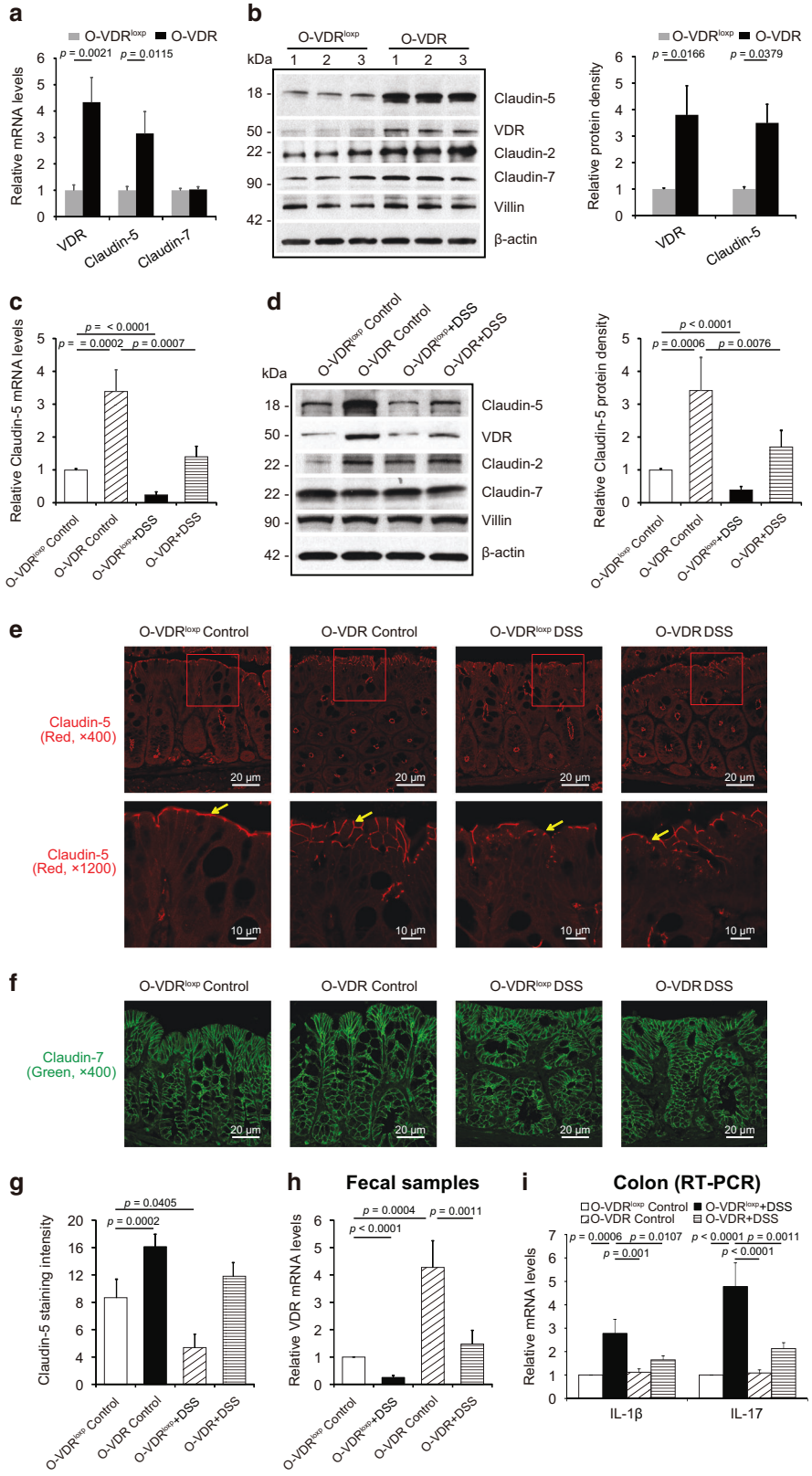

Intestinal permeability

Fluorescein Dextran (Molecular weight 3 kDa, diluted in HBSS) was gavaged (50 mg/g mouse). Four hours later, mouse blood samples were collected for fluorescence intensity measurement, as previously reported[44].

Immunofluorescence

Colonic tissues were freshly isolated and embedded in paraffin wax after fixation with 10% neutral buffered formalin. Immunofluorescence (IF) was performed on paraffin-embedded sections (4 μm), after preparation of the slides as described previously[59] followed by incubation for 1 h in blocking

Fig. 7 Overexpressed intestinal epithelial VDR led to increased Claudin-5 and reduced inflammation in vivo. a VDR overexpression in mice intestines increased Claudin-5 expression in the colon at mRNA and (**b**) protein levels (data are expressed as mean ± SD. $n = 3$, one-way ANOVA test). **c** Claudin-5 was minorly decreased at the mRNA and (**d**) protein levels in the intestinal tissue of O-VDR mice treatment with DSS compared to levels in the O-VDR^{loxp} mice (data are expressed as mean ± SD. $n = 3$, one-way ANOVA test). **e** Claudin-5 was minorly decreased in the intestinal tissue of O-VDR mice treated with DSS compared to levels in the O-VDR^{loxp} mice, according to immunofluorescence staining. Images are from a single experiment and represent five mice per group. **f** Claudin-7 was unchanged in the intestinal tissue of O-VDR mice treated with DSS compared to levels in the O-VDR^{loxp} mice according to immunofluorescence staining. Images are from a single experiment and represent five mice per group. **g** Intensity of the staining of Claudin-5. Images are from a single experiment and represent five mice per group. (Data are expressed as mean ± SD. $n = 5$, one-way ANOVA test). **h** VDR level in fecal samples was detected by RT-PCR. VDR expression was slightly decreased in O-VDR mice treated with DSS compared to O-VDR^{loxp} mice treated with DSS (data are expressed as mean ± SD. $n = 3$, one-way ANOVA test). **i** The inflammatory cytokines IL-1β and IL-17 were less increased in the DSS-induced O-VDR mice colitis model compared to the levels in O-VDR^{loxp} mice (data are expressed as mean ± SD. $n = 3$, one-way ANOVA test). All p values are shown in the figure.

solution (2% bovine serum albumin, 1% goat serum in HBSS) to reduce nonspecific background. The tissue samples were incubated overnight with primary antibodies at 4 °C. The following antibodies were used: anti-Claudin-5 and anti-Claudin-7. Slides were washed three times for 5 min each at room temperature in wash buffer. Samples were then incubated with secondary antibodies (goat anti-rabbit Alexa Fluor 488, Molecular Probes, CA; 1:200) for 1 h at room temperature. Tissues were mounted with SlowFade Antifade Kit (Life technologies, s2828, Grand Island, NY, USA), followed by a coverslip, and the edges were sealed to prevent drying. Specimens were examined with a Zeiss laser scanning microscope LSM 710 (Carl Zeiss Inc., Oberkochen, Germany).

Immunohistochemistry (IHC)

After preparation of the slides, antigen retrieval was achieved by incubating the slides for 15 min in hot preheated sodium citrate (pH 6.0) buffer and 30 min of cooling at room temperature. Endogenous peroxidases were quenched by incubating the slides in 3% hydrogen peroxide for 10 min, followed by three rinses with HBSS, and incubation for 1 h in 3% BSA + 1% goat serum in HBSS to reduce nonspecific background. Primary antibodies VDR (1:300) were applied for overnight in a cold room. After three rinses in HBSS, the slides were incubated in secondary antibody (1:100, Jackson ImmunoResearch Laboratories, Cat.No.115-065-174, West Grove, PA, USA) for 1 h at room temperature. After washing with HBSS for 10 min, the slides were incubated with vectastain ABC reagent (Vector Laboratories, Cat.No. PK-6100, Burlingame, CA 94010, USA) for 1 h. After washing with HBSS for 5 min, color development was achieved by applying a peroxidase substrate kit (Vector Laboratories, Cat.No. SK-4800, Burlingame, CA 94010) for 2–5 min, depending on the primary antibody. The duration of peroxidase substrate incubation was determined through pilot experiments and was then held constant for all of the slides. After washing in distilled water, the sections were counterstained with haematoxylin (Leica, Cat.No.3801570, Wetzlar, Germany), dehydrated through ethanol and xylene, and cover-slipped using a permount (Fisher Scientific, Cat.No.SP15-100, Waltham, MA, USA).

Real-time quantitative PCR

Total RNA was extracted from epithelial cell monolayers or mouse colonic epithelial cells using TRIzol reagent (Fisher Scientific, 15596026, Waltham, MA, USA). RNA reverse transcription was done using the iScript cDNA synthesis kit (Bio-Rad Laboratories, 1708891) according to the manufacturer's directions. The RT-cDNA reaction products were subjected to quantitative real-time PCR using the CFX96 Real-time PCR detection system (Bio-Rad Laboratories, Hercules, CA, USA) and iTaq™ Universal SYBR green supermix (Bio-Rad Laboratories, 1725121, Hercules, CA, USA) according to the manufacturer's directions. All expression levels were normalized to β-actin levels of the same sample. Percent expression was calculated as the ratio of the normalized value of each sample to that of the corresponding untreated control cells. All real-time PCR reactions were performed in triplicate. Primer sequences were designed using Primer-BLAST or were obtained from Primer Bank primer pairs listed in Table 1.

Chromatin immunoprecipitation (CHIP) assay

Binding of VDR to the Claudin-5 promoter was investigated using the ChIP assay as described previously[61]. Briefly, mouse colonic epithelial cells were collected by scraping the tissue from the colon of the mouse and the cells were treated with 1% formaldehyde for 10 min at 37 °C. Cells were washed twice in ice-cold phosphate-buffered saline containing protease inhibitor cocktail tablets. Cells were scraped into conical tubes, pelleted, and lysed in SDS Lysis Buffer. The lysate was sonicated to shear DNA into fragments of 200–1000 bp (4 cycles of 10 s sonication, 10 s pausing, Branson Sonifier 250, USA). The chromatin samples were pre-cleared with salmon sperm DNA-bovine serum albumin-sepharose beads then incubated overnight at 4 °C with VDR antibody. Immune complexes were precipitated with salmon sperm DNA-bovine serum albumin-sepharose beads. DNA was prepared by treatment with proteinase K, extraction with phenol and chloroform, and ethanol precipitation.

Identification of functional VDRE

PCR was used to construct the deletion of entire VDRE binding sites (ΔVDRE) and negative control (ΔD2/ΔD3) These fragments were separately subcloned into the firefly luciferase reporter plasmid pGL3-basic (Sequence see Supplement Fig. S2). Deletions of different domains of the Claudin-5 promoter cloned into the in pGL3 vector, driving luciferase expression, were transfected into SKCO15 cells. Luciferase activity in cell lysates was assayed by the Dual-Luciferase Reporter Assay System (Promega, Madison, WI, USA). Firefly luciferase activity was normalized to Renilla luminescence activity, and the activity was expressed as relative units.

Multiplex ELISA assay

A mouse-specific ProcartaPlex™ Multiplex Immunoassay plate from Invitrogen Thermo Fisher Scientific was used to detect serum cytokine levels. The assay was performed using the manufacturer's instruction manual using proper standards. Eventually, the plate was read using a Megpix Luminex machine.

Test fecal VDR by PCR

Total RNA was extracted from mouse fecal samples, as previously described[30]. Briefly, about 100 mg of frozen fecal pellet was used for RNA extraction using Trizol Reagent (Thermo Fisher Scientific, Cat.No.15596018, Waltham, MA, USA). To increase RNA yield in high quality, RNeasy minispin column (Qiagen, Cat No.217004, Hilden, Germany) was used by following the manufacturer's instructions.

Statistical analysis

All data were expressed as the mean ± SD. All statistical tests were two-sided. All p values < 0.05 were considered statistically significant. After the Shapiro–Wilk test confirmed that the data are normally distributed, the differences between samples were analyzed using unpaired Student's t test for two groups and one-way ANOVA for more than two groups as appropriate, respectively. The p values in ANOVA analysis were adjusted using the Tukey method to ensure accurate results. Pearson correlation analyses and scatter plots were conducted for staining intensity changes between VDR protein and Claudin-5, using SAS version 9.4 (SAS Institute, Inc., Cary, NC, USA) and R software (R Core Team (2021), R Foundation for Statistical Computing, Vienna, Austria). Other statistical analyses were performed using GraphPad Prism 6 (GraphPad, Inc., San Diego, CA., USA).

SUMMARY

What is already known about this subject

- Tight junction structures are essential in intestinal barrier integrity, inflammation, and cancer.
- Vitamin D deficiency and the vitamin D receptor (VDR) play important roles in the development of colon cancer.

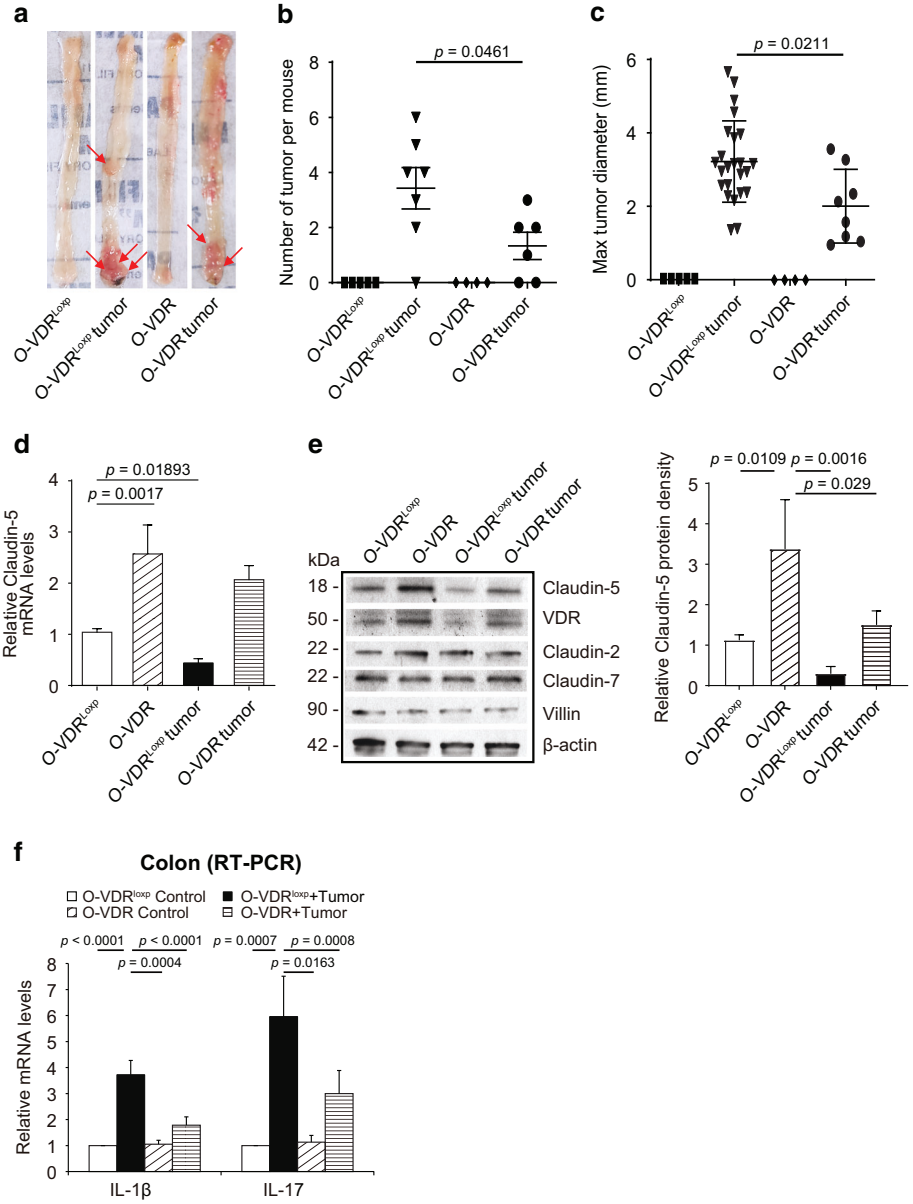

Fig. 8 Intestinal epithelial VDR overexpression mice have fewer and smaller tumors and show protection from decreased Claudin-5 and increased inflammation. a Colonic tumors in situ. Representative colons from different groups. Tumors were indicated by red arrows. **b** Tumor numbers in AOM-DSS induced colon cancer model: O-VDR^{loxp} and O-VDR mice (data are expressed as mean ± SD. $n = 4–7$, one-way ANOVA test). **c** Max tumor size in AOM-DSS induced colon cancer model: O-VDR^{loxp} and O-VDR mice (data are expressed as mean ± SD. $n = 4–7$, one-way ANOVA test). **d** Claudin-5 at the mRNA and (**e**) protein levels were decreased in the tumor tissue than in the control mice. O-VDR^{loxp} mice tumor tissue had much more decrease than the O-VDR mice (data are expressed as mean ± SD. $n = 3$, one-way ANOVA test). **f** The inflammatory cytokines IL-1β and IL-17 were less increased in the AOM/DSS-induced O-VDR mice colon cancer model, than the levels in O-VDR^{loxp} mice (data are expressed as mean ± SD. $n = 3$, one-way ANOVA test). All p values are shown in the figure.

What are the new findings

- Our study is the first to link barrier function, a specific tight junction protein, and genetic susceptibility through intestinal epithelial VDR in human CRC.
- Our study fills an existing gap by characterizing the mechanism of intestinal epithelial VDR in regulating barrier functions through alterations in TJs in tumorigenesis. VDR is important for maintaining the of physiological level of the TJ protein Claudin-5 in the colon. The *CLDN-5* gene is a downstream target of the VDR signaling pathway. Lack of VDR led to a reduction of Claudin-5 in tumors, whereas enhancing VDR increased Claudin-5 to protect the intestinal epithelial cells from tumorigenesis.
- We reported fecal VDR reduction in a colon cancer model. This introduces the possibility of identifying new biomarkers and therapeutic targets to restore VDR-dependent functions in CRC.

How might it impact clinical practice in the foreseeable future

- Diagnosis of CRC considering VDR status.
- Barrier functions and regulator as direct or indirect biomarkers.
- Intestinal barriers in cancer prevention and treatment.

Table 1. Real-time PCR primers.

Primers name	Sequence
mβ-actinF	5′-TGTTACCAACTGGGACGACA-3′
mβ-actinR	5′-CTGGGTCATCTTTTCACGGT-3′
mVDRF	5′-GAATGTGCCTCGGATCTGTGG-3′
mVDRR	5′-ATGCGGCAATCTCCATTGAAG-3′
mClaudin-5F	5′- AGGCACGGGTAGCACTCACG-3′
mClaudin-5R	5′- CATAGTTCTTCTTGTCGTAATC-3′
mClaudin-7F	5′-GCGACAACATCATCACAGCC-3′
mClaudin-7R	5′-CCTTGGAGGAATTGGACTTGG-3′
mTNF-α F	5′-CCCTCACACTCAGATCATCTTCT-3′
mTNF-α R	5′-GCTACGACGTGGGCTACAG-3′
mIL-1βF	5′-GCAACTGTTCCTGAACTCAACT-3′
mIL-1βR	5′-ATCTTTTGGGGTCCGTCAACT-3′
mIL-17F	5′-TTTAACTCCCTTGGCGCAAAA-3′
mIL-17R	5′-CTTTCCCTCCGCATTGACAC-3′
hβ-actinF	5′-AGAGCAAGAGAGGCATCCTC-3′
hβ-actinR	5′-CTCAAACATGATCTGGGTCA-3′
hVDRF	5′-GGACTGCCGCATCACCAA-3′
hVDRR	5′-TCATCTCCCGCTTCCTCT-3′
hClaudin-5F	5′-TTCGCCAACATTGTCGTCC-3′
hClaudin-5R	5′-TCTTCTTGTCGTAGTCGCCG-3′
hClaudin-7F	5′-CATCGTGGCAGGTCTTGCC-3′
hClaudin-7R	5′-GATGGCAGGGCCAAACTCATAC-3′

REFERENCES

1. Zeissig, S. et al. Changes in expression and distribution of claudin 2, 5 and 8 lead to discontinuous tight junctions and barrier dysfunction in active Crohn's disease. *Gut* **56**, 61–72 (2007).
2. Zhu, L. et al. Claudin Family Participates in the Pathogenesis of Inflammatory Bowel Diseases and Colitis-Associated Colorectal Cancer. *Front. Immunol.* **10**, 1441 (2019).
3. Cherradi, S., Martineau, P., Gongora, C. & Del Rio, M. Claudin gene expression profiles and clinical value in colorectal tumors classified according to their molecular subtype. *Cancer Manag. Res.* **11**, 1337–1348 (2019).
4. Haussler, M. R. et al. The nuclear vitamin D receptor: biological and molecular regulatory properties revealed. *J. Bone Miner. Res.* **13**, 325–349 (1998).
5. Xue, Y. & Fleet, J. C. Intestinal vitamin D receptor is required for normal calcium and bone metabolism in mice. *Gastroenterology* **136**, 1317–1327 (2009). e1311-1312.
6. Bouillon, R. et al. Vitamin D and human health: lessons from vitamin D receptor null mice. *Endocr. Rev.* **29**, 726–776 (2008).
7. Ogura, M. et al. Vitamin D3 modulates the expression of bile acid regulatory genes and represses inflammation in bile duct-ligated mice. *J. Pharm. Exp. Ther.* **328**, 564–570 (2009).
8. Kamen, D. L. & Tangpricha, V. Vitamin D and molecular actions on the immune system: modulation of innate and autoimmunity. *J. Mol. Med.* **88**, 441–450 (2010).
9. Waterhouse, J. C., Perez, T. H. & Albert, P. J. Reversing bacteria-induced vitamin D receptor dysfunction is key to autoimmune disease. *Ann. N. Y Acad. Sci.* **1173**, 757–765 (2009).
10. Liu, P. T., Krutzik, S. R. & Modlin, R. L. Therapeutic implications of the TLR and VDR partnership. *Trends Mol. Med.* **13**, 117–124 (2007).
11. Gombart, A. F., Borregaard, N. & Koeffler, H. P. Human cathelicidin antimicrobial peptide (CAMP) gene is a direct target of the vitamin D receptor and is strongly up-regulated in myeloid cells by 1,25-dihydroxyvitamin D3. *FASEB J.* **19**, 1067–1077 (2005).
12. Kong, J. et al. Novel role of the vitamin D receptor in maintaining the integrity of the intestinal mucosal barrier. *Am. J. Physiol. Gastrointest. Liver Physiol.* **294**, G208–216 (2008).
13. Adams, J. S. & Hewison, M. Unexpected actions of vitamin D: new perspectives on the regulation of innate and adaptive immunity. *Nat. Clin. Pr. Endocrinol. Metab.* **4**, 80–90 (2008).
14. Yu, S., Bruce, D., Froicu, M., Weaver, V. & Cantorna, M. T. Failure of T cell homing, reduced CD4/CD8alphaalpha intraepithelial lymphocytes, and inflammation in the gut of vitamin D receptor KO mice. *Proc. Natl. Acad. Sci. USA* **105**, 20834–20839 (2008).
15. Lloyd-Price, J. et al. Multi-omics of the gut microbial ecosystem in inflammatory bowel diseases. *Nature* **569**, 655–662 (2019).
16. Abreu, M. T. et al. Measurement of vitamin D levels in inflammatory bowel disease patients reveals a subset of Crohn's disease patients with elevated 1,25-dihydroxyvitamin D and low bone mineral density. *Gut* **53**, 1129–1136 (2004).
17. Lim, W. C., Hanauer, S. B. & Li, Y. C. Mechanisms of disease: vitamin D and inflammatory bowel disease. *Nat. Clin. Pr. Gastroenterol. Hepatol.* **2**, 308–315 (2005).
18. Wang, T. T. et al. Direct and indirect induction by 1,25-dihydroxyvitamin D3 of the NOD2/CARD15-defensin beta2 innate immune pathway defective in Crohn disease. *J. Biol. Chem.* **285**, 2227–2231 (2010).
19. Rufo, P. A. & Bousvaros, A. Current therapy of inflammatory bowel disease in children. *Paediatr. Drugs* **8**, 279–302 (2006).
20. Sun, J. Vitamin D and mucosal immune function. *Curr. Opin. Gastroenterol.* **26**, 591–595 (2010).
21. Song, M., Chan, A. T. & Jun, J. Influence of the Gut Microbiome, Diet, and Environment on Risk of Colorectal Cancer. *Gastroenterology* **158**, 322–340 (2020).
22. Lu, R. et al. Paneth cell alertness to pathogens maintained by vitamin D receptors. *Gastroenterology* **160**, 1269–1283 (2021).
23. Zhang, Y.-G. et al. Vitamin D receptor protects against dysbiosis and tumorigenesis via the JAK/STAT pathway in intestine. *Biorxiv* **02**, 2020.02.18.946335 (2020).
24. Zhang, Y. G. et al. Vitamin D Receptor Protects Against Dysbiosis and Tumorigenesis via the JAK/STAT Pathway in Intestine. *Cell Mol. Gastroenterol. Hepatol.* **10**, 729–746 (2020).
25. Wong, S. H. et al. Gavage of Fecal Samples From Patients With Colorectal Cancer Promotes Intestinal Carcinogenesis in Germ-Free and Conventional Mice. *Gastroenterology* **153**, 1621–1633 e1626 (2017).
26. Andoh, A. et al. Comparison of the fecal microbiota profiles between ulcerative colitis and Crohn's disease using terminal restriction fragment length polymorphism analysis. *J. Gastroenterol.* **46**, 479–486 (2011).
27. Bird, R. P. & Good, C. K. The significance of aberrant crypt foci in understanding the pathogenesis of colon cancer. *Toxicol. Lett.* **112-113**, 395–402 (2000).
28. Gudbjartsson, D. F. et al. Large-scale whole-genome sequencing of the Icelandic population. *Nat. Genet.* **47**, 435–444 (2015).
29. Kang, X. et al. Serrated neoplasia in the colorectum: gut microbiota and molecular pathways. *Gut Microbes* **13**, 1–12 (2021).
30. Yongguo Zhang, Y. X. & Sun, J. A simple and sensitive method to detect vitamin D receptor expression in various disease models using stool samples. *Genes Dis.* **8**, 939–945 (2020).
31. Wu, S. et al. Intestinal epithelial vitamin D receptor deletion leads to defective autophagy in colitis. *Gut* **64**, 1082–1094 (2015).
32. Sun, J. et al. Increased NF-kappaB activity in fibroblasts lacking the vitamin D receptor. *Am. J. Physiol. Endocrinol. Metab.* **291**, E315–322 (2006).
33. Kato, S. The function of vitamin D receptor in vitamin D action. *J. Biochem.* **127**, 717–722 (2000).
34. Zhang, Y.-G. et al. Tight junction CLDN2 gene is a direct target of the vitamin D receptor. *Sci. Rep.* **5**, 10642 (2015).
35. Capaldo, C. T. et al. Tight function zonula occludens-3 regulates cyclin D1-dependent cell proliferation. *Mol. Biol. Cell* **22**, 1677–1685 (2011).
36. Ivanov, A. I. et al. Microtubules regulate disassembly of epithelial apical junctions. *BMC Cell Biol.* **7**, 12 (2006).
37. Zhang, Y. G. et al. Intestinal epithelial HMGB1 inhibits bacterial infection via STAT3 regulation of autophagy. *Autophagy* **15**, 1935–1953 (2019).
38. Chatterjee, I. et al. Overexpression of Vitamin D Receptor in Intestinal Epithelia Protects Against Colitis via Upregulating Tight Junction Protein Claudin 15. *J. Crohn's Colitis.* **15**, 1720–1736 (2021).
39. Zhang, Y. G., Wu, S. & Sun, J. Vitamin D, Vitamin D Receptor, and Tissue Barriers. *Tissue Barriers* **1**, e23118 (2013).
40. Urashima, M. et al. Effect of Vitamin D Supplementation on Relapse-Free Survival Among Patients With Digestive Tract Cancers: the AMATERASU Randomized Clinical Trial. *JAMA* **321**, 1361–1369 (2019).
41. Vancamelbeke, M. & Vermeire, S. The intestinal barrier: a fundamental role in health and disease. *Expert Rev. Gastroenterol. Hepatol.* **11**, 821–834 (2017).
42. Mineta, K. et al. Predicted expansion of the claudin multigene family. *FEBS Lett.* **585**, 606–612 (2011).
43. Fujita, H. et al. Tight junction proteins claudin-2 and -12 are critical for vitamin D-dependent Ca2+ absorption between enterocytes. *Mol. Biol. Cell* **19**, 1912–1921 (2008).
44. Zhang, Y. G. et al. Lack of Vitamin D Receptor Leads to Hyperfunction of Claudin-2 in Intestinal Inflammatory Responses. *Inflamm. Bowel Dis.* **25**, 97–110 (2019).

45. Chen, H., Lu, R., Zhang, Y. G. & Sun, J. Vitamin D Receptor Deletion Leads to the Destruction of Tight and Adherens Junctions in Lungs. *Tissue Barriers* **6**, 1–13 (2018).
46. Turpin, W. et al. Increased Intestinal Permeability is Associated with Later Development of Crohn's Disease. *Gastroenterology*. **159**, 2092–2100 (2020).
47. Wong, S. H. & Yu, J. Gut microbiota in colorectal cancer: mechanisms of action and clinical applications. *Nat. Rev. Gastroenterol. Hepatol.* **16**, 690–704 (2019).
48. Pappa, H. M., Grand, R. J. & Gordon, C. M. Report on the vitamin D status of adult and pediatric patients with inflammatory bowel disease and its significance for bone health and disease. *Inflamm. Bowel Dis.* **12**, 1162–1174 (2006).
49. Zhang, J., Zhang, Y., Xia, Y. & Sun, J. Imbalance of the intestinal virome and altered viral-bacterial interactions caused by a conditional deletion of the vitamin D receptor. *Gut Microbes* **13**, 1957408 (2021).
50. Song, M., Chan, A. T. & Sun, J. Influence of the Gut Microbiome, Diet, and Environment on Risk of Colorectal Cancer. *Gastroenterology* **158**, 322–340 (2020).
51. Sun, J. & Kato, I. Gut microbiota, inflammation and colorectal cancer. *Genes Dis.* **3**, 130–143 (2016).
52. Sun, J. Impact of bacterial infection and intestinal microbiome on colorectal cancer development. *Chinese Med. J.* **135**, 400–408 (2022).
53. Galamb, O. et al. Inflammation, adenoma and cancer: objective classification of colon biopsy specimens with gene expression signature. *Dis. Markers* **25**, 1–16 (2008).
54. Sabates-Bellver, J. et al. Transcriptome profile of human colorectal adenomas. *Mol. Cancer Res.* **5**, 1263–1275 (2007).
55. Galamb, O. et al. Diagnostic mRNA expression patterns of inflamed, benign, and malignant colorectal biopsy specimen and their correlation with peripheral blood results. *Cancer Epidemiol. Biomark. Prev.:Publ. Am. Assoc. Cancer Res. Cosponsored Am. Soc. Preventive Oncol.* **17**, 2835–2845 (2008).
56. Pekow, J. et al. Gene signature distinguishes patients with chronic ulcerative colitis harboring remote neoplastic lesions. *Inflamm. Bowel Dis.* **19**, 461–470 (2013).
57. Zhang, Y.-G. et al. Lack of Vitamin D Receptor Leads to Hyperfunction of Claudin-2 in Intestinal Inflammatory Responses. *Inflamm. Bowel Dis.* **25**, 97–110 (2018).
58. Lu, R., Zhang, Y. G., Xia, Y. & Sun, J. Imbalance of autophagy and apoptosis in intestinal epithelium lacking the vitamin D receptor. *FASEB J.* **33**, 11845–11856 (2019).
59. Lu, R. et al. Chronic effects of a Salmonella type III secretion effector protein AvrA in vivo. *PLoS ONE* **5**, e10505 (2010).
60. Lu, R. et al. Alcohol Injury Damages Intestinal Stem Cells. *Alcohol. Clin. Exp. Res.* **41**, 727–734 (2017).
61. Wu, S., Xia, Y., Liu, X. & Sun, J. Vitamin D receptor deletion leads to reduced level of IkappaBalpha protein through protein translation, protein-protein interaction, and post-translational modification. *Int J. Biochem. Cell Biol.* **42**, 329–336 (2010).

ACKNOWLEDGEMENTS

We would like to thank Dr. David Zhou for assisting with the CRC human samples, Drs. Shaoping Wu and Rong Lu for assisting with the AOM/DSS model, and Jason S. Xia for proofreading.

AUTHOR CONTRIBUTIONS

Y.Z.: acquisition, analysis, and interpretation of data; drafting the paper; and statistical analysis. S.G.: assistance with western blots and TJ data. Y.X.: statistical analysis, and paper drafting. R.E.C.: Provided human biopsies and clinical perspective of CRC. J.S.: study concept and design, analysis and interpretation of data, writing the paper for important intellectual content, obtained funding, and study supervision.

FUNDING

This research was funded by the UIC Cancer Center, the NIDDK/National Institutes of Health grant R01 DK105118 and R01DK114126, VA Merit Award VA 1 I01 BX004824-01, and DOD BC160450P1 to Jun Sun. The study sponsors played no role in the study design, data collection, analysis, and interpretation of data. The contents do not represent the views of the United States Department of Veterans Affairs or the United States Government.

COMPETING INTERESTS

The authors declare no competing interests. The funders played no role in the study design, the collection, analyses, or interpretation of data, the writing of the paper, or the decision to publish the results.

ADDITIONAL INFORMATION

Supplementary information The online version contains supplementary material available at https://doi.org/10.1038/s41385-022-00502-1.

Correspondence and requests for materials should be addressed to Jun Sun.

Reprints and permission information is available at http://www.nature.com/reprints

Publisher's note Springer Nature remains neutral with regard to jurisdictional claims in published maps and institutional affiliations.